

**Supporting Information (SI)**

**The Relationship between Electron-transfer Coefficients of Oxygen Reduction Reaction  
Estimated from the Gibbs Free Energy of Activation and Butler-Volmer Equation**

Rajan Maurya, Rubul Das, Anand Kumar Tripathi and Manoj Neergat\*

*Department of Energy Science and Engineering  
Indian Institute of Technology Bombay (IITB), Powai, Mumbai-400076, India*

\*Corresponding author. Tel.: +91 22 2576 7893

Fax: +91 22 2276 4890

E-mail address: [nmanoj@iitb.ac.in](mailto:nmanoj@iitb.ac.in)

## 1.1 Voltammograms of the Pt electrode before and after recording the ORR polarization curves at various temperatures

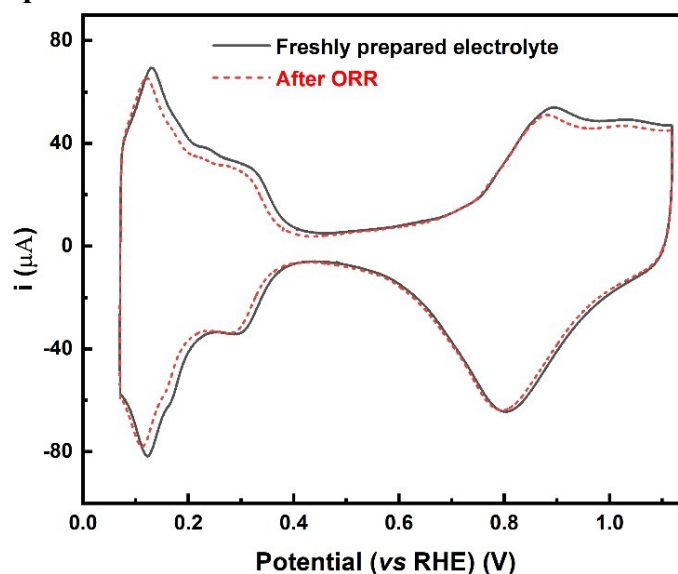


**Figure S1** Voltammograms of Pt black ( $\sim 51 \mu\text{g cm}^{-2}$ ) at room temperature in argon-saturated 0.1 M  $\text{HClO}_4$  at a scan rate of  $20 \text{ mV s}^{-1}$ , before and after recording ORR polarization curves at various temperatures (293 – 333 K).

The scan during ORR polarization was limited up to 1.05 V vs. RHE, and no prominent effect of temperature was observed on the surface structure or composition. It appears that the deviation in the data for different experiments at a given temperature mainly originates from the film making rather than the change in surface structure or composition. In the experimental temperature, potential and time range, the change in surface structure is negligible.

## 1.2 Conversion of the potential from $\text{Ag}/\text{AgCl}$ to reversible hydrogen electrode (RHE) scale

All the voltammograms are corrected for the non-zero pH using equation S1.

$$E (\text{vs. RHE}) = E(\text{vs. Ag/AgCl}) + 0.197 \text{ V} + 0.059 \times \text{pH} \quad (\text{S1})$$

### 1.3 Background voltammogram of Pt-black (0.1 M HClO<sub>4</sub>) at various temperatures

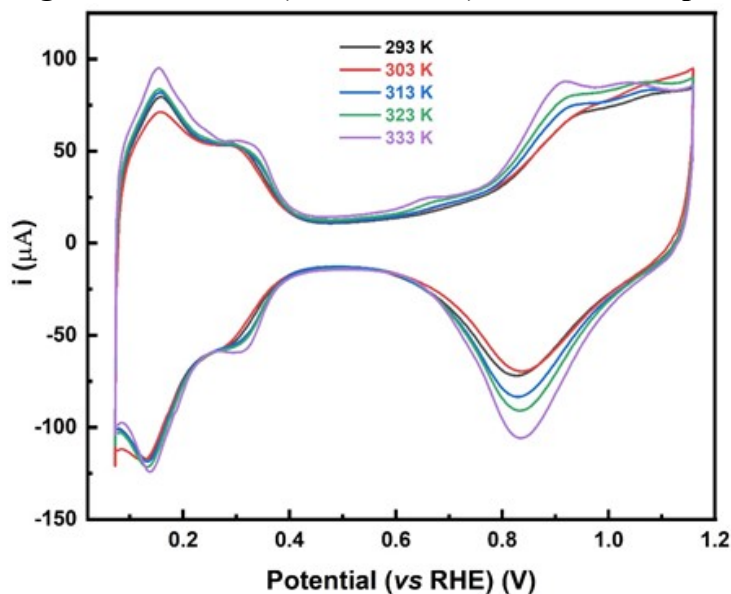


**Figure S2** Voltammograms of Pt black ( $\sim 51 \mu\text{g cm}^{-2}$ ) on a glassy-carbon rotating ring disk electrode (RRDE) in argon-saturated 0.1 M HClO<sub>4</sub> electrolyte recorded at a scan rate of 20 mV s<sup>-1</sup> in the temperature range of 293 – 333 K.

**Figure S2** shows the voltammograms of Pt black ( $\sim 51 \mu\text{g cm}^{-2}$ ) in argon-saturated 0.1 M HClO<sub>4</sub> in the temperature range of 293 – 333 K. After conditioning the electrode at room temperature (298 K) for 50 cycles, well-defined hydrogen underpotential adsorption/desorption ( $H_{\text{upd}}$ ) region (0 – 0.35 V), non-faradic double layer region (0.4 – 0.7 V), and oxide formation region (0.7 – 1.1 V) are observed in the voltammogram; these are widely reported typical polycrystalline platinum features.<sup>1-4</sup> With the increase in temperature, the voltammetric features remain almost the same, except for the slight rise in the surface coverage by the oxygenated species ( $\theta$ ) with temperature in the potential range of  $\sim 0.4 - 1.1$  V.

#### 1.4 Corrections to the ORR voltammogram for the background current, solution resistance, and mass-transport resistance

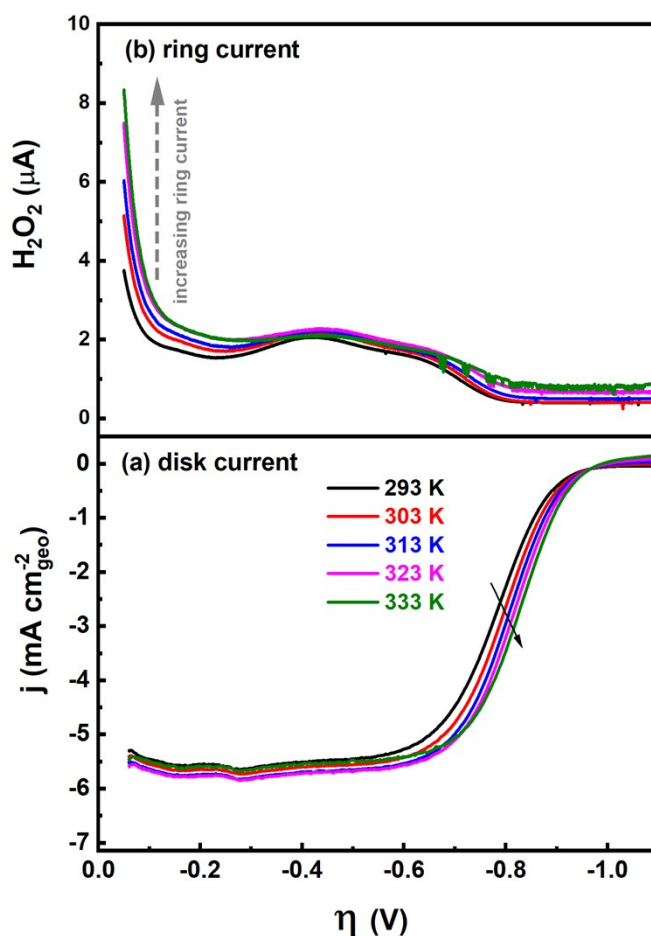


**Figure S3** Background corrected ORR voltammograms (disk currents ( $i_D$ )) (a) and corresponding ring current ( $I_R$ ) ( $H_2O_2$  oxidation current) (b) of Pt black ( $\sim 51 \mu g cm^{-2}$ ) on RRDE in oxygen-saturated 0.1 M  $H_2SO_4$  at a scan rate of  $20 mV s^{-1}$  in the positive sweep direction with 1600 rpm. The ring electrode potential is 1.23 V, and the collection efficiency is 0.2, in the temperature range of 293 – 333 K.

The ORR polarization curves (**Figure S3**) recorded at various temperatures are corrected for contributions from the background current (CV) and the solution resistance ( $R_s$ ). The background current correction is done by subtracting the voltammogram recorded in the supporting electrolyte (argon-saturated 0.1 M  $HClO_4$ ) (**Figure S2**) from the ORR voltammogram at the respective temperature. The  $R_s$  obtained from the electrochemical impedance spectra of ORR (not shown for convenience) is used to correct for the ohmic drop ( $iR_s$ ) using the following relation (equation S2).

$$E_{corr.} = E_{mea.} + (R_s \times i_{mea.}) \quad (S2)$$

Here,  $E_{corr.}$  is the potential corrected for the  $R_s$ ,  $E_{mea.}$  is the measured potential, and  $i_{mea.}$  is the measured current.

Koutecky-Levich equation used to correct for the mass-transport resistance is given by equation S3.

$$\frac{1}{i_{mea.}} = \frac{1}{i_k} + \frac{1}{i_d} \quad (S3)$$

Here,  $i_k$  is the kinetic current, and  $i_d$  is the diffusion-limited current. The  $i_k$  obtained from the  $i_{mea.}$  after correcting for background current,  $R_s$ , and mass-transport (**Figure S4**) is used for further analysis.

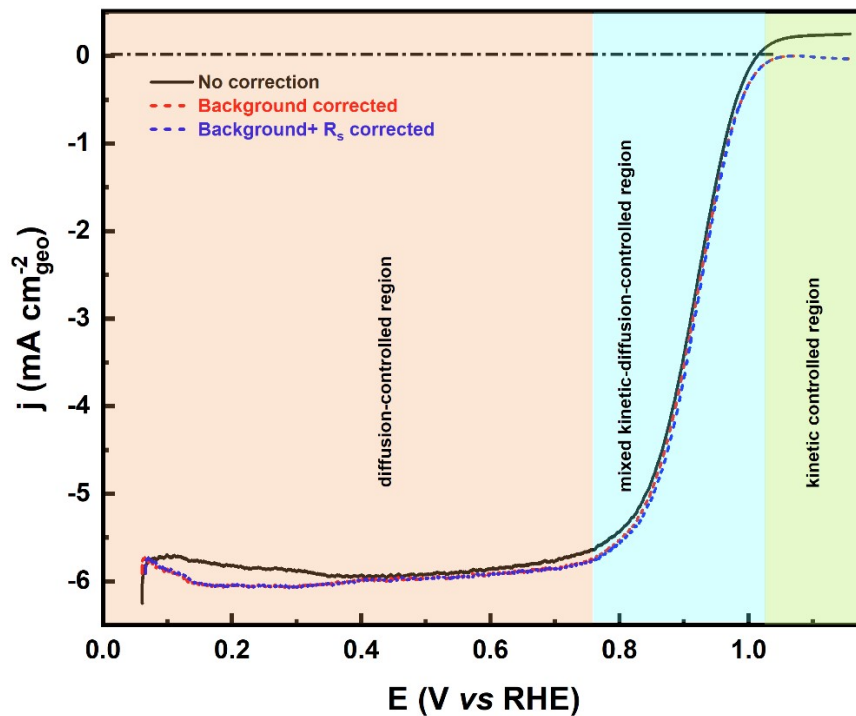


**Figure S4** The ORR voltammogram corrected for the background current (red line) and solution resistance (blue line).

## 2.1 The estimation of $\alpha$ from the B-V fitting

The  $i_k$  is analyzed by the B-V relation (equation S4).

$$i_k = i_0(e^{-\alpha f\eta} - e^{(1-\alpha)f\eta}) \quad (S4)$$

This form of the B-V equation accounts for the effect of applied  $\eta$  on both the forward (cathodic) and backward (anodic) reactions; the  $\eta$  range of analysis is high (0.3 – 0.4 V), and the effect of back reaction on the total current is negligible.

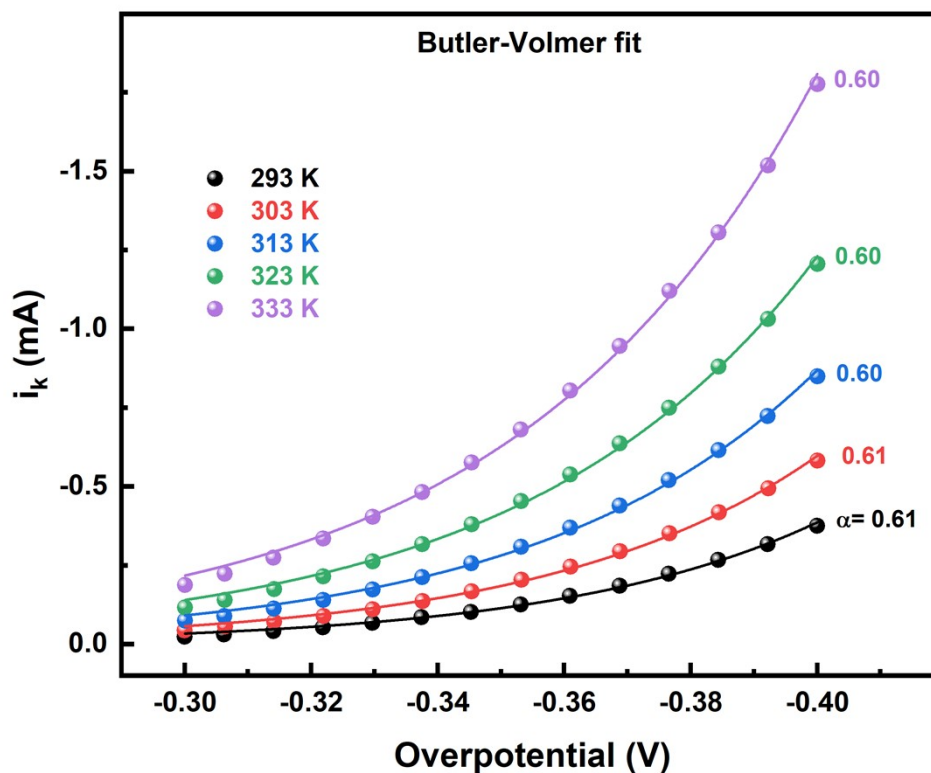


**Figure S5** The  $i_k$  vs.  $\eta$  of ORR of Pt black ( $\sim 51 \mu\text{g cm}^{-2}$ ) in 0.1 M  $\text{HClO}_4$  in the temperature range of 293 – 333 K. The symbols and solid lines show the experimental and the fitted data, respectively.

$\alpha$  is obtained by fitting the  $i_k$  with the B-V equation at various temperatures (**Figure S5**). The  $\alpha$  values obtained from the B-V fit are in the range of  $0.55 \pm 0.03$ .

**Table ST1**  $\alpha$  from the Tafel analysis and B-V fit in the temperature range of 293 – 333 K.

Temperature (K)	$\alpha$ (Tafel analysis)	$\alpha$ (B-V fit)
293	$0.60 \pm 0.03$	$0.58 \pm 0.01$
303	$0.62 \pm 0.02$	$0.59 \pm 0.01$
313	$0.63 \pm 0.04$	$0.55 \pm 0.02$
323	$0.63 \pm 0.04$	$0.54 \pm 0.03$
333	$0.62 \pm 0.04$	$0.55 \pm 0.02$

## 2.2 Estimation of instantaneous Tafel slope and instantaneous cathodic $\alpha_c$

The cathodic charge-transfer coefficient ( $\alpha_c$ ) is given by equation S5.<sup>5</sup>

$$\alpha_c = -\frac{RT \partial \ln(i_k)}{F \partial E} \quad (\text{S5})$$

The  $\alpha_c$  calculated from the instantaneous Tafel slope gives scattered values (**Figure S6**) but the average  $\alpha_c$  is  $\sim 0.7$  at all temperatures.

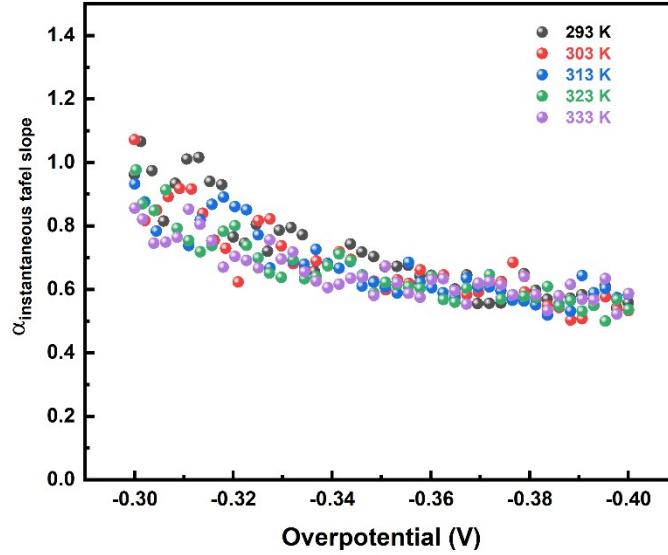


**Figure S6**  $\alpha_c$  (estimated from the instantaneous Tafel slope) vs.  $\eta$  plot at various temperatures.

### 2.3 Tafel analysis and estimation of the electrochemical charge-transfer coefficient ( $\alpha$ )

The relation between the  $i_k$  and the applied overpotential ( $\eta$ ) is given by the Butler-Volmer (B-V) relation (equation S6).

$$i_k = i_0 \left( e^{-\frac{\alpha F \eta}{RT}} - e^{\frac{(1-\alpha) F \eta}{RT}} \right) \quad (\text{S6})$$

Here,  $i_0$  is the exchange current. At large negative  $\eta$ , the cathodic current contribution in the B-V equation dominates, and the anodic current is negligible; that is  $\exp(-\alpha f \eta) \gg \exp((1-\alpha) f \eta)$ . Hence, equation S6 yields equation S7.

$$i_k = i_0 \exp\left(\frac{-\alpha F \eta}{RT}\right) \quad (\text{S7})$$

Taking log on both the sides and rearranging yields equation S8.

$$\eta = \frac{RT}{\alpha F} \ln(i_0) - \frac{RT}{\alpha F} \ln(i_k) \quad (\text{S8})$$

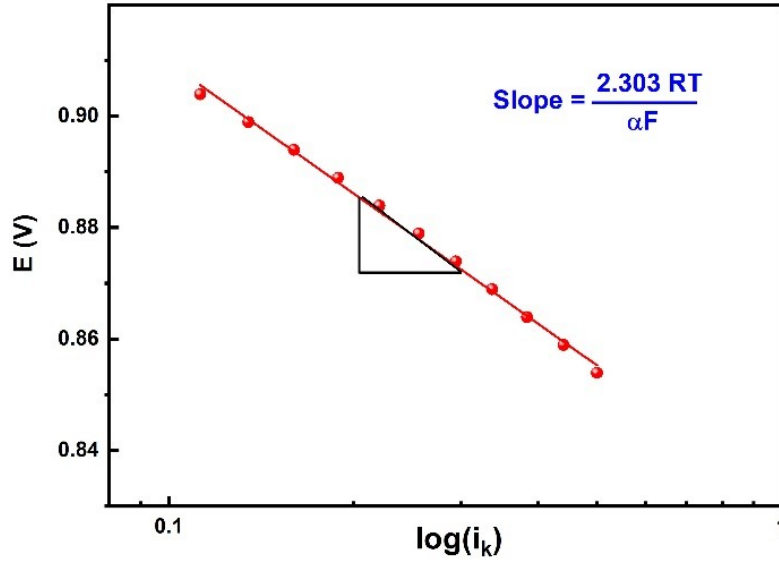


**Figure S7** Potential vs.  $\log(i_k)$  plot (Tafel plot).

Hence, plots of  $\eta$ /potential vs.  $\log(i_k)$  (Tafel plots) at various temperatures are used to estimate the  $\alpha$  at each temperature (equation S9).

$$\alpha = \frac{2.303 \times R \times T}{\text{slope} \times F} \quad (\text{S9})$$

### 3.1 Estimation of the activation enthalpy ( $\Delta H^\ddagger$ ) from the Eyring plot

The rate of any heterogeneous electrochemical reaction is given by equation S10.<sup>6</sup>

$$\text{Rate of reaction} = \frac{dN}{dt} = k[C] = \frac{i_k}{nFA} \quad (\text{S10})$$

$$k = \frac{i_k}{nFAC} \quad (\text{S11})$$

Here  $N$ ,  $k$ ,  $C$ , and  $A$  are the number of moles, the heterogeneous rate constant, the concentration of the dissolved reacting species ( $\text{mol cm}^{-3}$ ) and the area of the electrode, respectively.

Rate constant of a heterogeneous reaction is also given by Eyring relation (equation S12).

$$k = \frac{\kappa k_B T}{h} \exp\left(-\frac{\Delta G^\ddagger}{RT}\right) \quad (\text{S12})$$

Here,  $\Delta G^\ddagger$  is the Gibbs free energy. Moreover, equation S13 is obtained on accounting for the surface coverage ( $\theta$ ) by the adsorbed species.



$$k = \frac{\kappa k_B T (1 - \theta)}{h} \exp\left(-\frac{\Delta G^\ddagger}{RT}\right) \quad (\text{S13})$$

Thus,  $(1-\theta)$  is the fraction of the electrode surface available for the electrochemical reaction. Further  $\Delta G^\ddagger$  is defined by the equation S14.

$$\Delta G^\ddagger = \Delta H^\ddagger - T\Delta S^\ddagger \quad (\text{S14})$$

Here,  $\Delta H^\ddagger$  and  $\Delta S^\ddagger$  are the enthalpy of activation and entropy of activation, respectively. On substituting the equation S14 to equation S13 and comparing with equation S11 yields equation S15.

$$\frac{i_k}{T} = \frac{\kappa k_B n F A (1 - \theta) C}{h} \exp\left(\frac{\Delta S^\ddagger}{R}\right) \exp\left(-\frac{\Delta H^\ddagger}{RT}\right) \quad (\text{S15})$$

Taking log on both sides yields equation S16.

$$\frac{d(\log\left(\frac{i_k}{T}\right))}{d(1/T)} = \frac{1}{2.303} \ln\left(\frac{n F A C \kappa k_B (1 - \theta)}{h}\right) + \frac{\Delta S^\ddagger}{2.303 \times R} + \frac{(-\Delta H^\ddagger)}{2.303 \times R} \quad (\text{S16})$$

Thus,  $\Delta H^\ddagger$  at various overpotentials is estimated from the slope of Eyring plots ( $\log(i_k/T)$  vs.  $1/T$ ) (**Figure S8**). In principle, the intercept of the Eyring plot yields the  $\Delta S^\ddagger$  values.

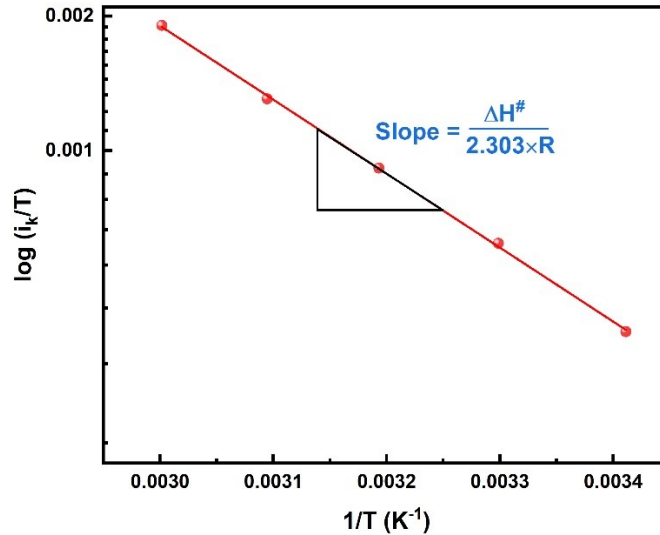


**Figure S8** Eyring plot used for the estimation of  $\Delta H^\ddagger$  ( $\log(i_k/T)$  vs.  $1/T$ ) at a given  $\eta$ .

The following relations (equation S17 and equation S18) are used to estimate the  $\Delta H^\ddagger$  and  $\Delta S^\ddagger$  from the Eyring plot.

$$\text{Slope} = \frac{-\Delta H^\ddagger}{2.303 \times R} \quad (\text{S17})$$

$$\text{Intercept } (A_f) = \frac{1}{2.303} \ln \left( \frac{nFA(1-\theta)C_{O_2} \kappa k_B}{h} \right) + \frac{\Delta S^\ddagger}{2.303 \times R} \quad (\text{S18})$$

### 3.2 Enthalpic contribution of the charge-transfer coefficient ( $\alpha_H$ )

The enthalpic contribution of the  $\alpha$  to the total  $\alpha$  is obtained from  $\Delta H^\ddagger$  vs.  $\eta$  plot. The slope of  $\Delta H^\ddagger$  vs.  $\eta$  plot is given by the equation S19.

$$\text{slope} = \frac{\alpha_H \times F}{1000} \quad (\text{S19})$$

$$\alpha_H = \frac{\text{slope} \times 1000}{F} \quad (\text{S20})$$

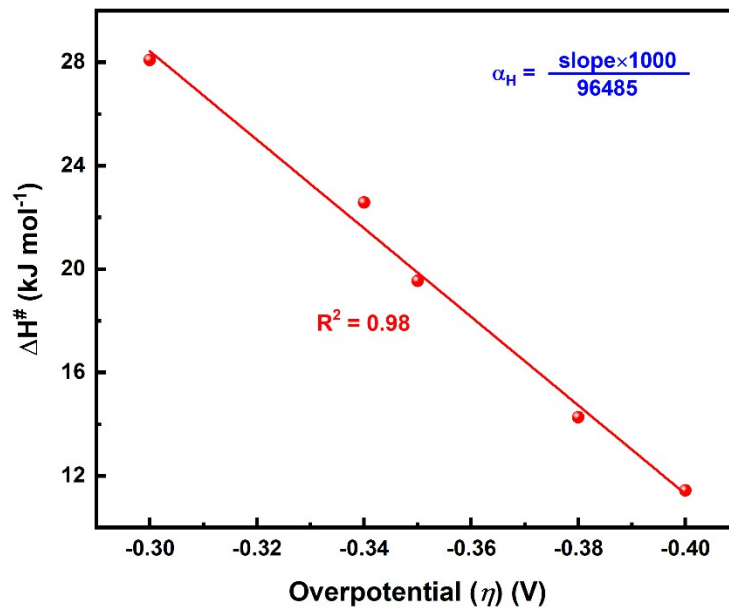


**Figure S9**  $\Delta H^\ddagger$  vs.  $\eta$  plot for ORR on Pt black ( $\sim 51 \mu\text{g cm}^{-2}$ ) in 0.1 M  $\text{HClO}_4$ .

### 3.3 Entropic contribution of the charge-transfer coefficient ( $\alpha_S$ )

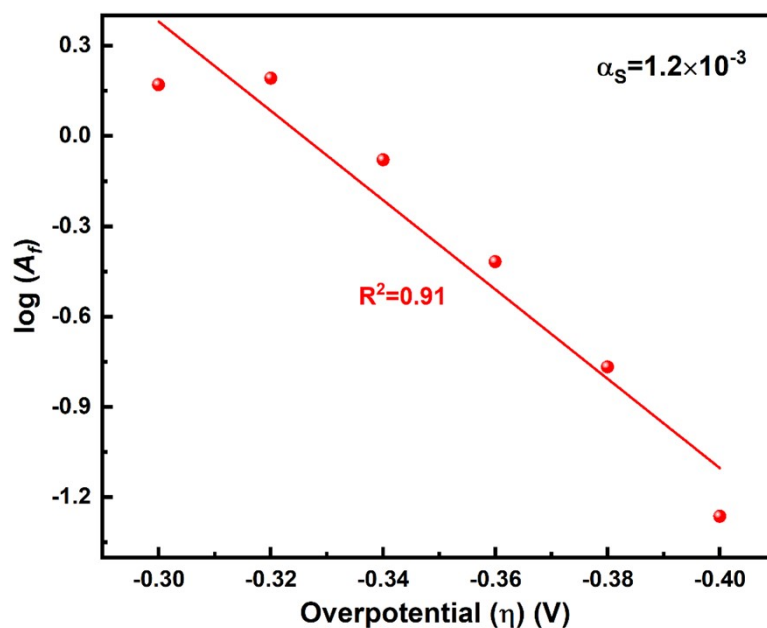


**Figure S9**  $\log(A_f)$  vs.  $\eta$  plot for ORR on Pt black ( $\sim 51 \mu\text{g cm}^{-2}$ ) in 0.1 M  $\text{HClO}_4$ .

Except the  $\Delta S^\ddagger$  and  $\theta$  values in the equation S18, all the other quantities remain constant with temperature and potential. Therefore, the plot of intercept of the Eyring plot ( $A_f$ ) vs.  $\eta$  is used to estimate the  $\alpha_S$ . As explained in Section 3.4, the slope of the  $\log(A_f)$  vs.  $\eta$  hence  $\alpha_S$  does not change much after correcting the  $A_f$  for the surface coverage ( $1-\theta$ ). The slope of  $\log(A_f)$  vs.  $\eta$  is given by equation S21.

$$\text{slope} = \frac{\alpha_S \times F}{R} \quad (\text{S21})$$

$$\alpha_S = \frac{\text{slope} \times R}{F} \quad (\text{S22})$$

The total  $\alpha$  of heterogeneous electrochemical reaction is also given by equation S23.

$$\alpha = \alpha_H + T\alpha_S \quad (\text{S23})$$

**Table ST2**  $\alpha_S$  and  $T\alpha_S$  at 313 K, estimated at various electrodes

Slope	$\alpha_S (\times 10^{-3})$	$T\alpha_S$	$R^2$
-17.5	-1.5	-0.47	0.94
-19.4	-1.6	-0.52	0.95
-14.8	-1.2	-0.39	0.91
-21	-1.8	-0.56	0.98
-10.5	-0.9	-0.28	0.85

### 3.4 Effect of surface coverage on the pre-exponential factor ( $A_f$ )

The effect of  $\theta$  is contained in the pre-exponential term of the Eyring relation (equation S24).

$$\frac{i_k}{T} = \frac{\kappa k_B n F A (1 - \theta) C_{O_2}}{h} \exp\left(\frac{\Delta S^\ddagger}{R}\right) \exp\left(-\frac{\Delta H^\ddagger}{RT}\right) \quad (S24)$$

$$\frac{d(\log\left(\frac{i_k}{T}\right))}{d(1/T)} = \frac{1}{2.303} \ln\left(\frac{n F A C_{O_2} \kappa k_B}{h}\right) + \frac{1}{2.303} \ln(1 - \theta) + \frac{\Delta S^\ddagger}{2.303 \times R} + \frac{(-\Delta H^\ddagger)}{2.303 \times R}$$

(S25)

Since the  $\theta$  is estimated from the voltammograms at various temperatures, equation S25 is used to account for the  $\theta$ . The  $A_f$  vs.  $\eta$  slope does not change after accounting for the  $\theta$  (**Fig. S11**).

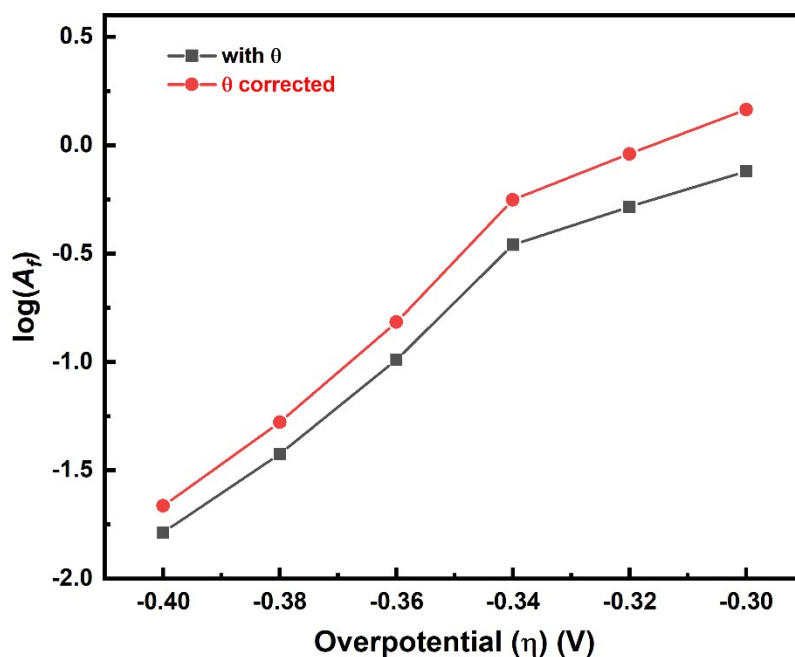


**Figure S10**  $\log(A_f)$  vs.  $\eta$  plot for ORR on Pt black ( $\sim 51 \mu\text{g cm}^{-2}$ ) in 0.1 M  $\text{HClO}_4$ , red line represents the data corrected for  $\theta$ .

### 3.5 Illustration of electrochemical and electrocatalytic processes by Eyring plots at various overpotentials

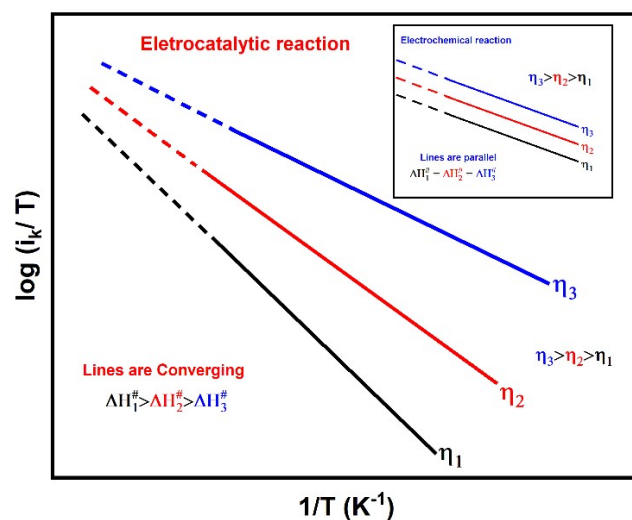


**Figure S11** Schematic of the Eyring plots at various overpotentials for electrochemical (inset) and electrocatalytic reactions.

### 3.6 Theoretical limiting current density at rotating disk electrode (RDE)

Diffusion-limited current density ( $j_d$ ) of the reaction in a rotating disk electrode (RDE) configuration is given by the Levich relation (equation S26).

$$j_{d,RDE} = 0.62nFC_0D^{2/3}\nu^{-1/6}\omega^{1/2} \quad (S26)$$

For ORR at 293 K,  $n$  (4),  $F$  ( $96485 \text{ C mol}^{-1}$ ),  $C_0$  ( $1.26 \times 10^{-6} \text{ mol cm}^{-3}$ ),  $D$  ( $1.93 \times 10^{-5} \text{ cm}^2 \text{ s}^{-1}$ ),  $\nu$  ( $0.01009 \text{ cm}^2 \text{ s}^{-1}$ ),  $\omega$  ( $1600 \text{ rpm} = 167.5 \text{ rps}$ ) are the number of electrons transferred, Faraday constant, concentration of the dissolved oxygen, diffusion coefficient of the oxygen, kinematic viscosity, and angular velocity, respectively.

Putting these values in equation S26.

$$j_{d,RDE} = 0.62 \times 4 \times 96485 \times 1.26 \times 10^{-6} \times (1.93 \times 10^{-5})^{2/3} \times (0.01009)^{-1/6} \times (167.5)^{1/2}$$

$$j_{d,RDE} = 6.034 \text{ mA cm}^{-2}$$

### 3.7 Temperature dependence of the $j_d$

$j_d$  of an electrochemical reaction in a RDE configuration is given by Levich relation (equation S26). It is decided by the temperature-dependent diffusion coefficient of  $O_2$  ( $D_{O_2}$ ) in the electrolyte and kinematic viscosity ( $\nu$ ).

Temperature-dependence of the  $D_{O_2}$  in the aqueous electrolyte is given by equation S27.

$$D_{O_2} \propto \frac{T}{\eta} \quad (S27)$$

The relation between the ratio of dynamic viscosity ( $\eta$ ) and the electrolyte density ( $\rho$ ) is given by equation S28.

$$\nu = \frac{\eta}{\rho} \quad (S28)$$

Also, for an open system, the sum of the partial pressures is the total pressure of 1 bar (equation S29).

$$P_{O_2} + P_{H_2O} = 1 \quad (S29)$$

Using equations S26, S27, S28, and S29, then rearranging yields equation S30<sup>2</sup>.

$$j_{d,T} \propto \frac{T^{2/3} \rho^{1/6}}{\eta^{5/6}} C_{O_2} (1 - P_{H_2O}) = P_T C_{O_2} (1 - P_{H_2O}) \quad (S30)$$

Normalizing the temperature-dependent  $j_d$  with  $j_d$  at 20°C temperature gives equation S31.

$$\frac{j_{d,T}}{j_{d,20}} = \frac{P_T C_T (1 - P_{H_2O}(T))}{P_{(20^\circ C)} C_{(20^\circ C)} (1 - P_{H_2O}(20^\circ C))} \quad (S31)$$

Here,  $C_T$  is the total pressure of dissolved oxygen at temperature T, and  $P_T$  is the total pressure. It is assumed that the temperature dependence of viscosity, solubility of  $O_2$ , and acid density are the same as those for pure water.

Based on the above relations, the  $j_d$  up to 318 K is predicted to be constant; and then it decreases with increase in temperature<sup>2</sup>. At higher temperatures, such decrease in  $j_d$  is attributed to a significant rise in the electrolyte partial pressure.

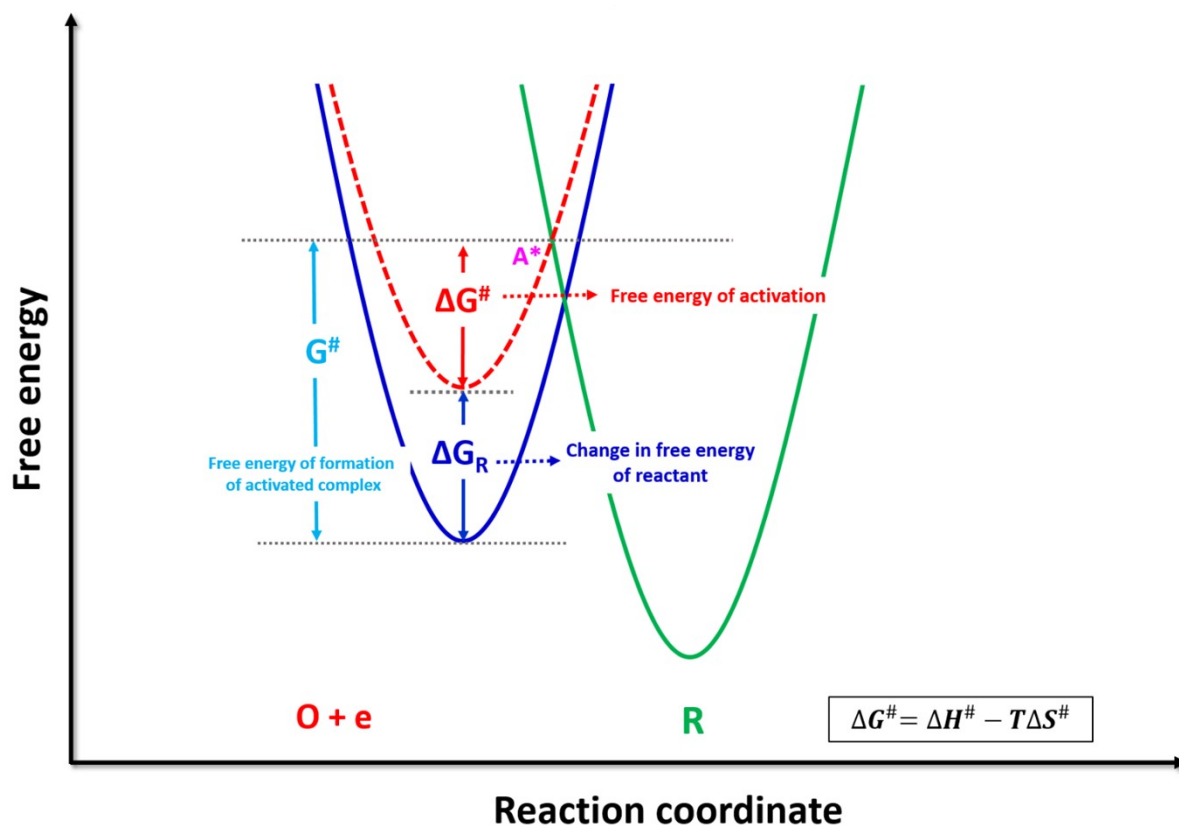


**Figure S12** Schematic of energy surface diagram for Gibbs Free Energy/activation enthalpies referred in the main manuscript.

### References

1. N. M. Marković, T. J. Schmidt, B. N. Grugr, H. A. Gasteiger, R. J. Bhém and P. N. Ross, Effect of temperature on surface processes at the Pt(111) - liquid interface: Hydrogen adsorption, oxide formation, and CO oxidation. *J. Phys. Chem. B*, 1999, **103**, 8568–8577
2. U. A. Paulus, T. J. Schmidt, H. A. Gasteiger and R. J. Behm, Oxygen reduction on a high-surface area Pt/Vulcan carbon catalyst: A thin-film rotating ring-disk electrode study. *J. Electroanal. Chem.*, 2001, **495**, 134–145
3. R. Gómez, J. M. Feliu and H. D. Abruña, Induced adsorption of chloride and bromide by submonolayer amounts of copper underpotentially deposited on Pt(111). *J. Phys. Chem.*, 1994, **98**, 5514–5521
4. R. Devivaraprasad, T. Kar, P. Leuaa and M. Neergat, Recovery of active surface sites of shape-controlled platinum nanoparticles contaminated with halide ions and its effect on surface-

structure. *J. Electrochem. Soc.*, 2017, **164**, H551–H560

5. R. Guidelli, R. G. Compton, J. M. Feliu, E. Gileadi, J. Lipkowski, W. Schmickler and S. Trasatti, Definition of the transfer coefficient in electrochemistry (IUPAC Recommendations 2014). *Pure Appl. Chem.*, 2014, **86**, 259–262
6. A. J. Bard and L. R. Faulkner, *Electrochemical Methods Fundamentals and Applications*. vol. 8 (John Wiley & Sons, Inc., 2015).